Two- to one-dimensional transition of self-assembled coordination networks at surfaces by organic ligand addition

Alexander Langner,[a] Steven L. Tait,*[ab] Nian Lin,[ac] Rajadurai Chandrasekar,†[d] Mario Ruben[d] and Klaus Kern[ae]

Received (in Berkeley, CA, USA) 15th December 2008, Accepted 17th March 2009
First published as an Advance Article on the web 2nd April 2009
DOI: 10.1039/b822476e

Two-dimensional metal–organic coordination networks at a Cu(100) surface are transformed to a new supramolecular structure with one-dimensional coordination character by the addition of a second organic ligand.

Rational design and structural control of highly-ordered nanometre-scale frameworks are fundamental ambitions of supramolecular assembly research in solution-based systems,[1–3] and more recently, for the efficient ''bottom-up'' nanopatterning of surfaces.[4–6] We demonstrate a transition from two-dimensional to one-dimensional organization in a surface-supported supramolecular assembly, triggered by the addition of a second ligand to the system. A structural reorganization from a homotopic, two-dimensional coordination network into 1D coordination chains is triggered by the addition of terephthalic acid. The possibility to tailor the structure and function of such systems is of great interest for a wide variety of applications, including host–guest systems[7,8] and growth templates.[9,10] The self-organization of highly regular, extended structural domains requires supramolecular interactions that are selective, directional, and non-covalent (*i.e.*, reversible for error correction), such as hydrogen bonding or metal–ligand complexation. Two-dimensional metal–organic coordination networks (2D-MOCN) have been demonstrated with design control over size,[11,12] nanopore aspect ratio,[13] geometry,[14,15] and adsorptive activity.[8] The higher level of complexity in some of these systems[13,15,16] is achieved through multi-ligand mixtures, which may be critical for full realization of sophisticated, hierarchically organized surface architectures for designable chemical function and physical properties.

In this paper we demonstrate a further level of control in the design of 2D-MOCN systems. We present a transition from a stable 2D coordination network[17] to a 1D coordination structure with low coordination number, triggered by the addition of a second ligand to the system. The added ligand orders and stabilizes the final cooperative assembly *via* hydrogen bonding. Whereas prior reports of co-crystallization[16,18] improved stability and order, the mixed molecular phase reported here is particularly interesting since it is preferred to the homotopic alternatives, which are individually stable.

For this purpose, 4,4′-bis(4-pyridyl)(2,2′-bipyrimidine) (PBP, Scheme 1),[17] a linear aromatic molecule with 4-pyridyl end groups and a 2,2′-bipyrimidine backbone, was chosen. In the presence of Cu atoms, PBP self-organizes directly in thermally stable and extended 2D metal–organic coordination networks on Cu(100) (Fig. 1), Ag(100), and Ag(111) surfaces.[17] On each of these surfaces, differing in lattice constant and symmetry, the same robust coordination geometry is observed: bidentate coordination of two nitrogen atoms of the bipyrimidine moiety of one ligand to a Cu atom and the pyridyl end group of another ligand attaching perpendicular to the first (see molecular model in Fig. 1).

In this work, the bipyrimidine PBP (synthesized according to ref. 17) and terephthalic acid (TPA, Scheme 1, Fluka Chemie GmbH, >99% purity) are sequentially evaporated under ultra high vacuum (UHV) conditions onto an atomically flat Cu(100) single-crystal surface, which has been cleaned by standard sputtering–annealing procedure.[16] Due to the sequential deposition, the PBP–Cu structure will form on the surface before TPA deposition, according to previous work, which demonstrated formation of that structure immediately upon room temperature deposition.[17] Subsequent deposition of the TPA triggers a transformation to the structures reported here. The sample is subsequently annealed to 400 K to allow efficient mixing and assembly. In the absence of TPA, this annealing step would allow ripening of the PBP–Cu structure.[17]

The sample is characterized *in situ* using a home-built scanning tunnelling microscope at room temperature. It has been demonstrated previously that the carboxylic acid groups of TPA deprotonate during the adsorption or subsequent annealing on Cu(100),[19,20] leaving carboxylate moieties which are excellent electron acceptors for the intermolecular hydrogen-bond-type interactions described below. The UHV environment enables detailed analysis of the structures using

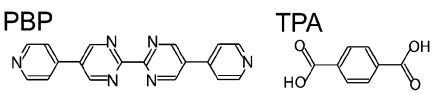

Scheme 1

[a] *Max Planck Institute for Solid State Research, Heisenbergstrasse 1, D-70569, Stuttgart, Germany*
[b] *Department of Chemistry, Indiana University, Bloomington, IN 47405, USA. E-mail: tait@indiana.edu; Fax: +1 812 855 8300; Tel: +1 812 855 1302*
[c] *Department of Physics, The Hong Kong University of Science and Technology, Clear Water Bay, Kowloon, Hong Kong, China*
[d] *Institute of Nanotechnology, Karlsruhe Institute of Technology, PF 3640, D-76021, Karlsruhe, Germany*
[e] *Institute de Physiques des Nanostructures, Ecole Polytechnique Fédérale de Lausanne, CH-1015, Lausanne, Switzerland*
† *Present address*: School of Chemistry, University of Hyderabad, Central University Post, Gachi Bowli, Hyderabad 500046, India

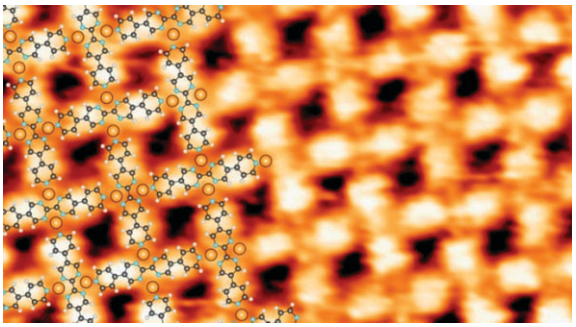

Fig. 1 High-resolution STM image (8.2 nm × 4.6 nm) of thermally stable open pore coordination network of PBP on Cu(100), superimposed with molecular model. Image reproduced from ref. 17 with permission from Wiley-VCH.

surface analysis methods (especially local structural characterization with scanning probes) and also allows a high degree of experimental control, especially with regard to surface composition and temperature.[21]

Fig. 2a, an STM topograph overview recorded at room temperature shows that the codeposition of PBP and TPA onto Cu(100) results in highly ordered and extended domains of a mixed phase of both molecules. The yield of this structure is quantitative, *i.e.*, limited by the smaller of the surface coverage of either PBP or TPA. Experiments were performed with either an excess of PBP or of TPA, the mixed phase in Fig. 2 is again found in quantitative yield and the excess molecule forms separate homoligand domains. In the mixed phase structure of Fig. 2, the PBP ligands form parallel 1D rows, which are interconnected by the shorter TPA molecules, fixing the well-defined periodic spacing between the pyridyl rows to 15.8 Å ± 0.1 Å (measured by STM). Four rotational domain orientations are observed by STM, where the coordination chain direction (indicated by dashed lines in Fig. 2a) is ±23° from the [011] or [0$\bar{1}$1] principle directions of the substrate (arrows in Fig. 2a).

The close-up in the inset of Fig. 2a, shows that these rows consist of individual PBP molecules lined up with a segment spacing of 19.5 Å ± 0.1 Å. Considering the length of the PBP "building blocks" as 15.4 Å, the gap between pyridyl moieties of adjacent PBP molecules facing each other, can be determined as 4.1 Å, which is too large for direct stable interaction. However, this distance is in very good agreement with the previously reported linear N–Cu–N coordination node stabilizing 1D Cu–bipyridyl coordination rows.[14] In addition, in the STM data, bright round protrusions can be observed in the intersection of neighboring PBP molecules along these rows, displaying the position of Cu coordination centers.

Neighboring bipyrimidine chains are bridged by three TPA molecules per PBP ligand, *i.e.* in a segment of 19.5 Å. Notably, the spacing between adjacent TPA molecules is significantly compressed compared to their homotopic hydrogen-bonded phase (three TPA molecules in a segment of 23.0 Å in Cu(100)-(3 × 3)-TPA structure).[22] Along with that compression, we observe that the distance between neighboring Cu–PBP rows (15.8 Å) is larger than observed for the Cu–bipyridyl chains (15.3 Å) in similar cases, where TPA interacted purely *via* hydrogen bonds.[16] Another notable

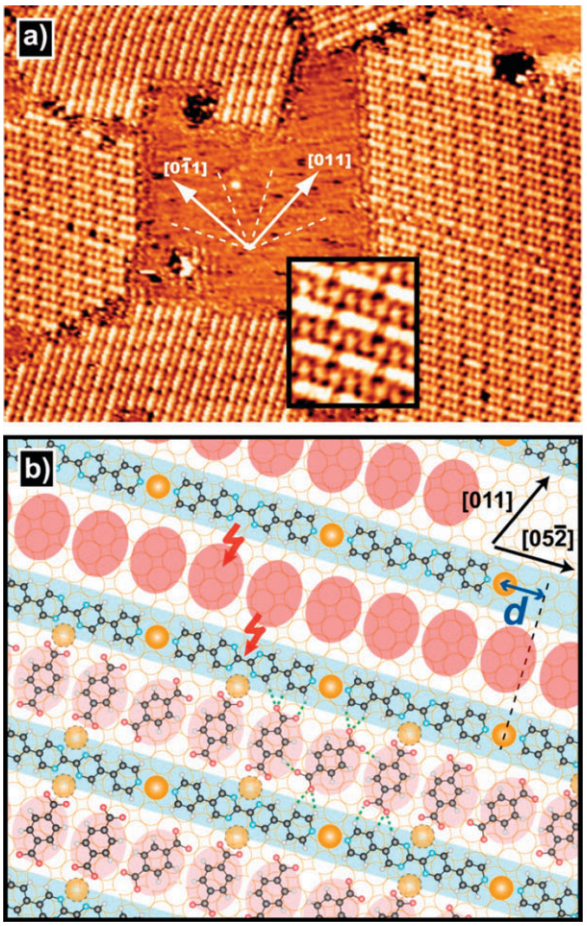

Fig. 2 (a) STM topograph (49 nm × 35 nm) of the hybrid phase of PBP and TPA on Cu(100) with different possible domain orientations, indicated by white dashed lines. The PBP molecules are forming linear Cu–pyridyl coordination chains, interconnected by TPA molecules. Inset: close-up image of structure (5.0 nm × 5.8 nm). (b) Tentative molecular model of the PBP–TPA mixed phase. The upper part reflects the information deduced directly from the STM data, where the red ovals represent TPA molecules. In the lower part, Cu centers in the proximity of the bipyrimidine side groups and the possible configuration of the TPA molecules are added to the model in the most likely supramolecular arrangement, as discussed in the main text.

structural difference is the orientation of the coordination chains along the [05$\bar{2}$] direction of the surface here rather than the low index directions as found in the prior study. The compression along the TPA rows, broadening between the rows, and reorientation compared to the previous work with 4,4′-bis(4-pyridyl)biphenyl ligands[10] indicate a different bonding geometry, due to the presence of the bipyrimidine backbone here. Although the STM does not provide direct characterization of the intermolecular interactions and coordination bonding, insight into the formation of these structures can be gained by careful analysis of the data.

A molecular model of the assembly superimposed on a Cu(100) substrate is shown in Fig. 2b. As deduced from the STM data, the bipyrimidine chains are turned by 23° in respect to the [011] direction of the substrate (running in [05$\bar{2}$] direction, indicated by dashed lines in Fig. 2a), which allows commensurability of the segments with the substrate, *i.e.* the

Cu centers and the bipyrimidine molecules are always in the same position relative to the substrate. Considering the spacing between neighboring chains, their lateral displacement $d = 4.2 \pm 0.5$ Å (measured by STM, see Fig. 2b) and the substrate geometry suggests that this is not only the case along the coordination chains, but that all PBP molecules and Cu centers, in the same domain, have an identical position relative to the substrate, as depicted in the model.

The relative position of the Cu centers and ligands with respect to the substrate atoms cannot be determined unambiguously from the STM data, since atomic resolution of the network and the substrate at the same time was not achieved. The red ovals in the upper part of Fig. 2b, depict the position of the bridging TPA molecules, as determined from the STM data, but the exact orientation of the individual TPA molecules at these positions is not clear.

In the bottom part of Fig. 2b we depict the TPA more explicitly in order to provide a speculative model, in our view the most likely, for the TPA bonding and orientation. In two out of three TPA positions, one carboxylate group faces a bipyrimidine group of the pyridyl chain (indicated by a red lightning bolt), which would be repulsive in the case of direct bonding due to the negative charge density on each of the functional groups. In the homoligand phase of PBP, these bipyrimidine side groups are attractive for chelate coordination of Cu atoms, while a second pyridyl molecule attaches perpendicularly *via* a pyridyl group forming a three-fold N–Cu coordination (see Fig. 1). In the tentative part of the molecular model (lower part of Fig. 2b) it is proposed that a Cu atom is coordinated similarly in the bipyrimidine side group in the PBP–TPA mixed phase, allowing a TPA ligand to attach by chelation. This TPA molecule could interact with an adjacent bipyrimidine chain *via* hydrogen bonding (indicated by the dashed green line), bridging both rows. Interestingly, with the $[05\bar{2}]$ structure orientation, these Cu atoms could all sit in energetically favorable hollow sites of the Cu(100) substrate. In this model, the coordination bonds are all set to 2.0 Å, while the hydrogen bonds are between 2.0 Å and 2.5 Å, which are consistent with reported values for studies at surfaces[23–26] and in solution.[27] While two TPA molecules are interacting with the Cu centers at the sides of the bipyrimidine backbones of PBP, the third TPA molecule, which appears tilted in the STM data compared to the others, seems to be solely interacting *via* hydrogen bonds, stabilizing the pyridyl chains as well as the two TPA neighbors. In this configuration the third TPA molecule maximizes its hydrogen bonds, while the distances to the Cu centers inside the pyridyl rows are too large to form coordination bonds in any possible orientation. Although the exact orientation of the TPA molecules is not unambiguously determined from the data, we think that the model described above is the most likely scenario.

We have demonstrated that by codeposition, the TPA molecules "passivate" the side groups of the PBP ligands and prevent the growth of a 2D homotopic coordination network of the PBP ligand. The TPA drives the PBP into parallel 1D coordination chains, which are regularly arranged with a well defined separation determined by the bridging TPA molecules. Such transformative, cooperative assembly is a valuable tool for structural control in 2D supramolecular assembly, which can even reduce the coordination dimensionality of the assembly. This strategy in the toolkit of rational 2D supramolecular assembly will contribute to the current rapid development of functional supramolecular architectures at surfaces.

Notes and references

1 J. M. Lehn, *Supramolecular Chemistry. Concepts and Perspectives*, VHC, Weinheim, Germany, 1995.
2 P. J. Stang and B. Olenyuk, *Acc. Chem. Res.*, 1997, **30**, 502–518.
3 M. C. T. Fyfe and J. F. Stoddart, *Acc. Chem. Res.*, 1997, **30**, 393–401.
4 J. A. Theobald, N. S. Oxtoby, M. A. Phillips, N. R. Champness and P. H. Beton, *Nature*, 2003, **424**, 1029–1031.
5 S. Furukawa, H. Uji-i, K. Tahara, T. Ichikawa, M. Sonoda, F. C. DeSchryver, Y. Tobe and S. DeFeyter, *J. Am. Chem. Soc.*, 2006, **128**, 3502–3503.
6 W. Xiao, X. Feng, P. Ruffieux, O. Gröning, K. Müllen and R. Fasel, *J. Am. Chem. Soc.*, 2008, **130**, 8910–8912.
7 M. Blunt, X. Lin, M. D. Gimenez-Lopez, M. Schroder, N. R. Champness and P. H. Beton, *Chem. Commun.*, 2008, 2304–2306.
8 S. Stepanow, M. Lingenfelder, A. Dmitriev, H. Spillmann, E. Delvigne, N. Lin, X. B. Deng, C. Z. Cai, J. V. Barth and K. Kern, *Nat. Mater.*, 2004, **3**, 229–233.
9 R. Madueno, M. T. Raisanen, C. Silien and M. Buck, *Nature*, 2008, **454**, 618–621.
10 S.-S. Li, H.-J. Yan, L.-J. Wan, H.-B. Yang, B. H. Northrop and P. J. Stang, *J. Am. Chem. Soc.*, 2007, **129**, 9268–9269.
11 U. Schlickum, R. Decker, F. Klappenberger, G. Zoppellaro, S. Klyatskaya, M. Ruben, I. Silanes, A. Arnau, K. Kern, H. Brune and J. V. Barth, *Nano Lett.*, 2007, **7**, 3813–3817.
12 S. Stepanow, N. Lin, J. V. Barth and K. Kern, *J. Phys. Chem. B*, 2006, **110**, 23472–23477.
13 A. Langner, S. L. Tait, N. Lin, C. Rajadurai, M. Ruben and K. Kern, *Proc. Natl. Acad. Sci. U. S. A.*, 2007, **104**, 17927–17930.
14 S. L. Tait, A. Langner, N. Lin, S. Stepanow, C. Rajadurai, M. Ruben and K. Kern, *J. Phys. Chem. C*, 2007, **111**, 10982–10987.
15 N. Lin, A. Langner, S. L. Tait, C. Rajadurai, M. Ruben and K. Kern, *Chem. Commun.*, 2007, 4860–4862.
16 A. Langner, S. L. Tait, N. Lin, R. Chandrasekar, M. Ruben and K. Kern, *Angew. Chem., Int. Ed.*, 2008, **47**, 8835–8838.
17 S. L. Tait, A. Langner, N. Lin, R. Chandrasekar, O. Fuhr, M. Ruben and K. Kern, *ChemPhysChem*, 2008, **9**, 2495–2499.
18 Y. Wang, M. Lingenfelder, T. Classen, G. Costantini and K. Kern, *J. Am. Chem. Soc.*, 2007, **129**, 15742–15743.
19 S. Stepanow, T. Strunskus, M. Lingenfelder, A. Dmitriev, H. Spillmann, N. Lin, J. V. Barth, C. Woll and K. Kern, *J. Phys. Chem. B*, 2004, **108**, 19392–19397.
20 S. L. Tait, Y. Wang, G. Costantini, N. Lin, A. Baraldi, F. Esch, L. Petaccia, S. Lizzit and K. Kern, *J. Am. Chem. Soc.*, 2008, **130**, 2108–2113.
21 S. L. Tait, *ACS Nano*, 2008, **2**, 617–621.
22 M. A. Lingenfelder, H. Spillmann, A. Dmitriev, S. Stepanow, N. Lin, J. V. Barth and K. Kern, *Chem.–Eur. J.*, 2004, **10**, 1913–1919.
23 S. Stepanow, N. Lin, F. Vidal, A. Landa, M. Ruben, J. V. Barth and K. Kern, *Nano Lett.*, 2005, **5**, 901–904.
24 F. Vidal, E. Delvigne, S. Stepanow, N. Lin, J. V. Barth and K. Kern, *J. Am. Chem. Soc.*, 2005, **127**, 10101–10106.
25 G. Pawin, K. L. Wong, D. Kim, D. Sun, L. Bartels, S. Hong, T. S. Rahman, R. Carp and M. Marsella, *Angew. Chem., Int. Ed.*, 2008, **47**, 8442–8445.
26 G. Pawin, K. L. Wong, K. Y. Kwon and L. Bartels, *Science*, 2006, **313**, 961–962.
27 T. Steiner, *Angew. Chem., Int. Ed.*, 2002, **41**, 48–76.